Physics of the Earth and Planetary Interiors 220 (2013) 73–78 (reprint)

Contents lists available at SciVerse ScienceDirect

Physics of the Earth and Planetary Interiors

journal homepage: www.elsevier.com/locate/pepi

Short communication

The December 7, 2012 Japan Trench intraplate doublet (M_w 7.2, 7.1) and interactions between near-trench intraplate thrust and normal faulting

Thorne Lay [a,*], Zacharie Duputel [b], Lingling Ye [a], Hiroo Kanamori [b]

[a] Department of Earth and Planetary Sciences, University of California Santa Cruz, Santa Cruz, CA 95064, USA
[b] Seismological Laboratory, California Institute of Technology, Pasadena, CA 91125, USA

ARTICLE INFO

Article history:
Received 11 April 2013
Received in revised form 29 April 2013
Accepted 30 April 2013
Available online 16 May 2013
Edited by: George Helffrich

Keywords:
Japan Trench intraplate earthquake doublet
Plate bending stress
Earthquake triggering

ABSTRACT

A pair of large earthquakes ruptured within the Pacific plate below the Japan Trench about 14 s apart on December 7, 2012. The doublet began with an M_w 7.2 thrust event 50–70 km deep, followed by an M_w 7.1–7.2 normal-faulting event in the range 10–30 km deep about 27 km to the south–southwest. The deep lithosphere thrust earthquake is the largest such event to be recorded seaward of the rupture zone of the great March 11, 2011 Tohoku M_w 9.0 earthquake. It follows an extensive intraplate normal-faulting aftershock sequence since 2011 extending up to 100 km east of the trench. Many small normal faulting aftershocks of the doublet occurred along a 60 km-long trench-parallel-trend beneath the inner trench slope. The complex overlapping signals produced by the doublet present challenges for routine long-period moment tensor inversion procedures, but the inadequacy of any single point-source inversion was readily evident from comparisons of different data sets and solutions using different frequency bands. We use a two double-couple inversion of W-phase signals to quantify the doublet characteristics, along with an iterative deconvolution of P-wave signals that extracts a compatible three sub-event sequence. The occurrence of a large deep compressional event near the trench several years subsequent to a great megathrust event is similar to a sequence that occurred in the central Kuril Islands between 2006 and 2009, and appears to be associated with stress changes caused by the preceding interplate thrusting and intraplate normal faulting. Recent large deep compressional events in the Philippine Trench and northern Kermadec Trench regions may be influenced by strain accumulation on adjacent locked interplate megathrusts. Regions having more pronounced curvature of the subducting plate may have unrelaxed bending stresses, facilitating occurrence of large deep thrust faulting in advance of future megathrust failures, as was observed in 1963 in the central Kuril Islands region but not in the gently curving Pacific plate offshore of the great Tohoku event.

1. Introduction

Large thrust events located within subducting plates seaward of megathrust plate boundaries are relatively rare. These earthquakes have been observed to precede large interplate ruptures in several regions, suggesting that they may involve accumulation of in-plate strain associated with a locked megathrust during the interplate seismic cycle superimposed on the plate bending strain environment (e.g., Christensen and Ruff, 1988; Lay et al., 1989). Whereas several very large normal faulting events have occurred seaward of regions with weak seismic coupling, this is not the case for large thrust events. Four large intraplate thrust events have occurred at depths of 40–60 km offshore of subduction zones in the past 4 years, two following great underthrusting ruptures, at odds with earlier observations. All four events involve sequences with shallow normal faulting and some level of interplate thrust-faulting, suggestive of strong stress change interactions between diverse fault systems in the shallow subduction zone environment.

On December 7, 2012 a large earthquake occurred below the Japan Trench (08:18:23 UTC, 37.890°N 143.949°E, 31 km depth, m_b 7.2, M_S 7.3, M_e 8.3, M_{ww} 7.3, http://comcat.cr.usgs.gov/earthquakes/eventpage/pde20121207081823130_31#summary). Rapidly produced USGS point-source focal mechanisms indicated intraplate thrust faulting solutions that differed in dip and depth (35–58 km) between W-phase, surface wave, and body wave solutions, as also found by other groups (e.g., http://outreach.eri.u-tokyo.ac.jp/eqvolc/20121207sanrikueq/eng/). Given the unusual occurrence of a large near-trench thrust event seaward of an earlier great megathrust rupture, we examined this event, finding that it is comprised of two distinct ruptures with different fault geometries and source depths. We resolve the faulting complexity and consider the implications of the near-trench intraplate thrust faulting relative to the other recent observations of this category of earthquake.

* Corresponding author.
E-mail address: tlay@ucsc.edu (T. Lay).

0031-9201/$ - see front matter © 2013 Elsevier B.V. All rights reserved.
http://dx.doi.org/10.1016/j.pepi.2013.04.009

2. The 2012 Japan Trench intraplate doublet

The two fault geometries that ruptured during the December 7, 2012 earthquake are indicated by the large focal mechanisms in Fig. 1, as determined below. Also shown are the two-sub-event moment tensor solutions produced by the global Centroid-Moment Tensor (gCMT) project (http://www.globalcmt.org/CMTsearch.html). Li and Ji (2013) also determined a two-subevent source model, as did the Earthquake Research Institute of the University of Tokyo (http://outreach.eri.u-tokyo.ac.jp/eqvolc/20121207sanrikueq/eng/). Best double-couples from regional centroid moment tensor inversions by the Japanese National Research Institute for Earth Science and Disaster Prevention (NIED) are shown for the mainshock (single-event inversion) and for smaller aftershocks that occurred over the next few months, plotted at the regional CMT centroid locations. The NIED centroid location for the mainshock is about 30 km oceanward of the USGS National Earthquake Information Center (NEIC) location, and the moment tensor indicates normal faulting, in contrast to the USGS thrust-faulting point-source solutions. The NIED centroid locations for smaller events tend to be located landward by ~15 km relative to the USGS NEIC locations (inset) although individual events can have 20–30 km differences in location estimate. This is similar to range of differences for location estimate found for JMA hypocenters of outer trench slope events compared to hypocenters using ocean bottom seismometer deployments (e.g., Hino et al., 2009; Obana et al., 2012). Huang and Zhao (2013) find a similar mislocation tendency for JMA estimates relative to relocations using a 3D structure.

Our own single-event point source moment tensor inversion of global low frequency (1.67 to 5 mHz) W-phase signals for the mainshock (Kanamori and Rivera, 2008) is shown in Fig. 2a, and is consistent with the USGS W-phase inversion. The moment tensor has significant non-double couple component with a best-double couple that is a thrust mechanism with one steeply dipping-plane. While this solution fits the W-phase signals adequately (examples are shown in Fig. 2a), it was apparent that the following long-period surface wave motions were poorly predicted, and this

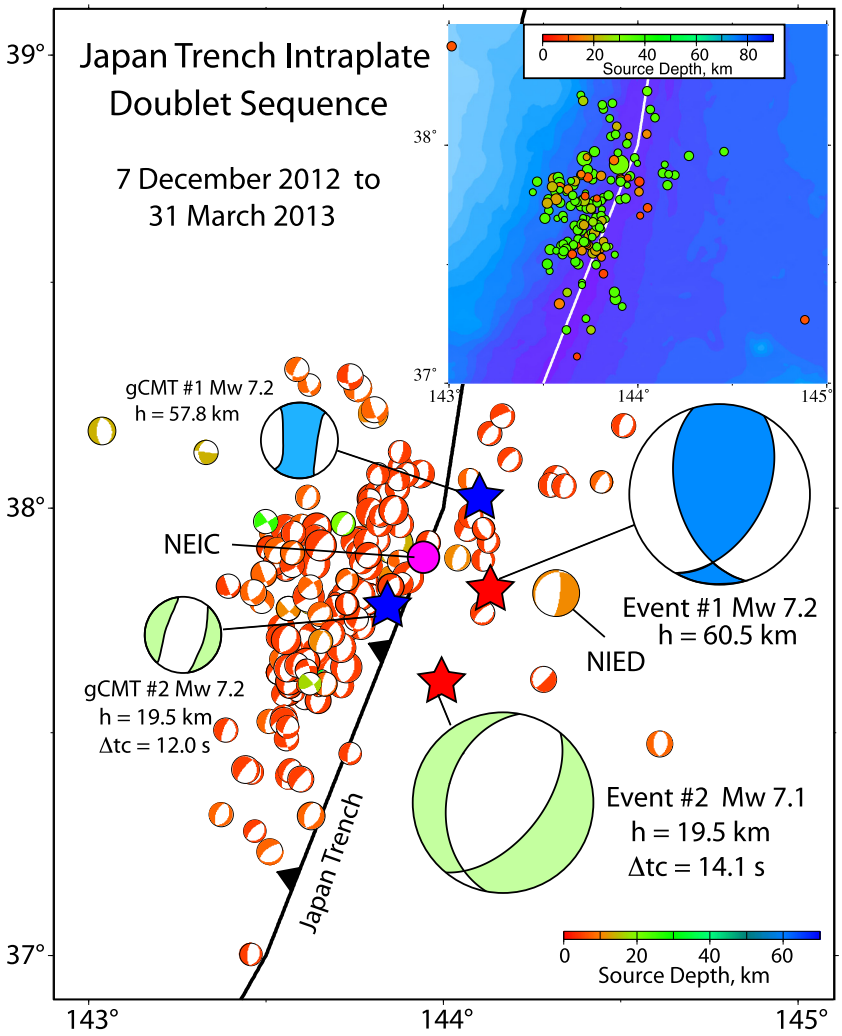

Fig. 1. The 2012 Japan Trench intraplate sequence comprising a large earthquake doublet on 7 December 2012 and aftershock activity through 29 March 2013. The inset map shows the USGS NEIC locations for the mainshock and aftershocks. The position of the Japan Trench is indicated by the barbed line. The red stars indicate point-source locations for the two double-couple W-phase inversion for the doublet. The two largest mechanisms indicate the associated faulting geometries, h is centroid depth, and Δtc is the difference in centroid times. Corresponding doublet moment tensor solutions from the global Centroid Moment Tensor (gCMT) are shown along with their centroid locations (blue stars). The magenta dot is the USGS epicenter. The mechanism labeled NIED is the best double-couple for a single-event regional centroid moment tensor inversion (NIED CMT) and smaller focal mechanisms are NIED CMT best-double couples for the aftershock sequence, all plotted at the CMT centroid locations, with symbol size proportional to M_w. Colors indicate source depth.

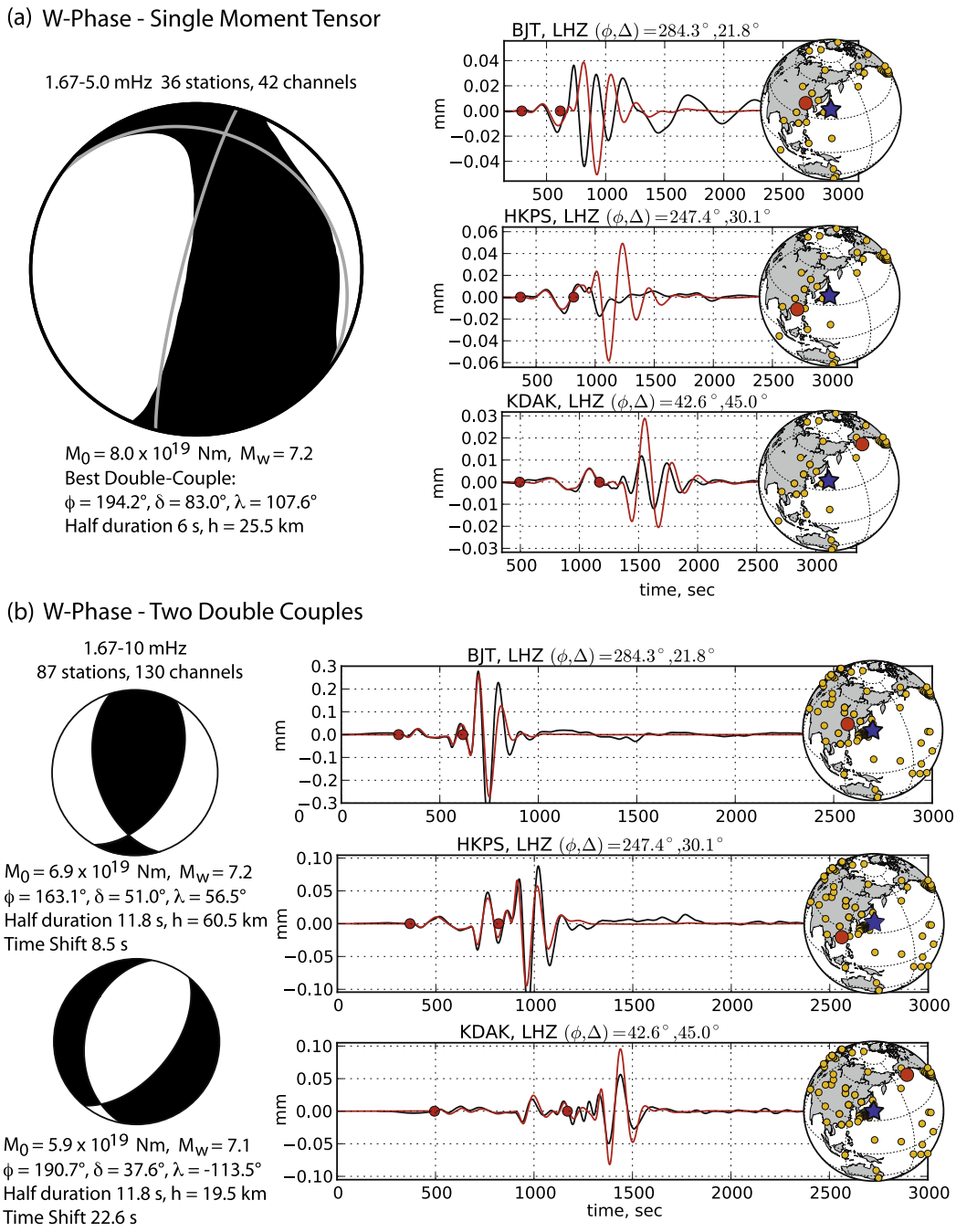

Fig. 2. (a) Single point-source moment tensor W-phase inversion solution for the December 7, 2012 event, using 42 records in the 1.67–5.0 mHz passband. Strike (φ), dip (δ) and rake (λ) are indicated for the best double-couple decomposition. Representative data (black) and synthetic (red) waveforms are shown on the right, with the red dots delimiting the W-phase signal. The inset maps indicate the positions of the epicenter (blue star), particular station (red dot), and other stations used in the inversion (gold dots). Note the poor prediction of the waveforms of later arriving fundamental mode surface waves. (b) Two double-couple W-phase inversion solution for the December 7, 2012 event, using 130 records in the 1.67–10 mHz passband. Representative data and synthetic waveforms are shown on the right. Note the improved prediction of the surface wave signals that arrive after the W-phase windows. Additional waveform comparisons for this inversion are shown in Fig. S1.

leads to discrepancies with centroid moment tensor point-source inversions. Inconsistency with P wave first-motions (see Fig. 3a) further suggested faulting complexity that could not be represented with a single point-source moment tensor.

Using a two double-couple parameterization of the W-phase inversion (Duputel et al., 2012) and a larger number of traces with the broadened passband 1.67–10 mHz yielded the solution in Figs. 1 and 2b. This involves an initial thrust faulting subevent with a centroid depth of 60.5 km and a seismic moment of 6.9×10^{19} Nm (M_w 7.2), followed 14.1 s later by a normal faulting sub-event at centroid depth 19.5 km with a seismic moment of 5.9×10^{19} Nm (M_w 7.1) located 27 km to the south–southwest. The difference in depth prevents the long-period motions from canceling for these reversed geometries; for events of equal moment and reversed mechanisms at least 30 km of depth difference is required to match the amplitudes of the data in the passband used in the multiple event inversion. The fit to the W-phase signals in the broadened passband is very good, and the prediction of the following surface wave signals is quite close to observations even for the extended passband (Fig. 2b and Supplementary Fig. S1).

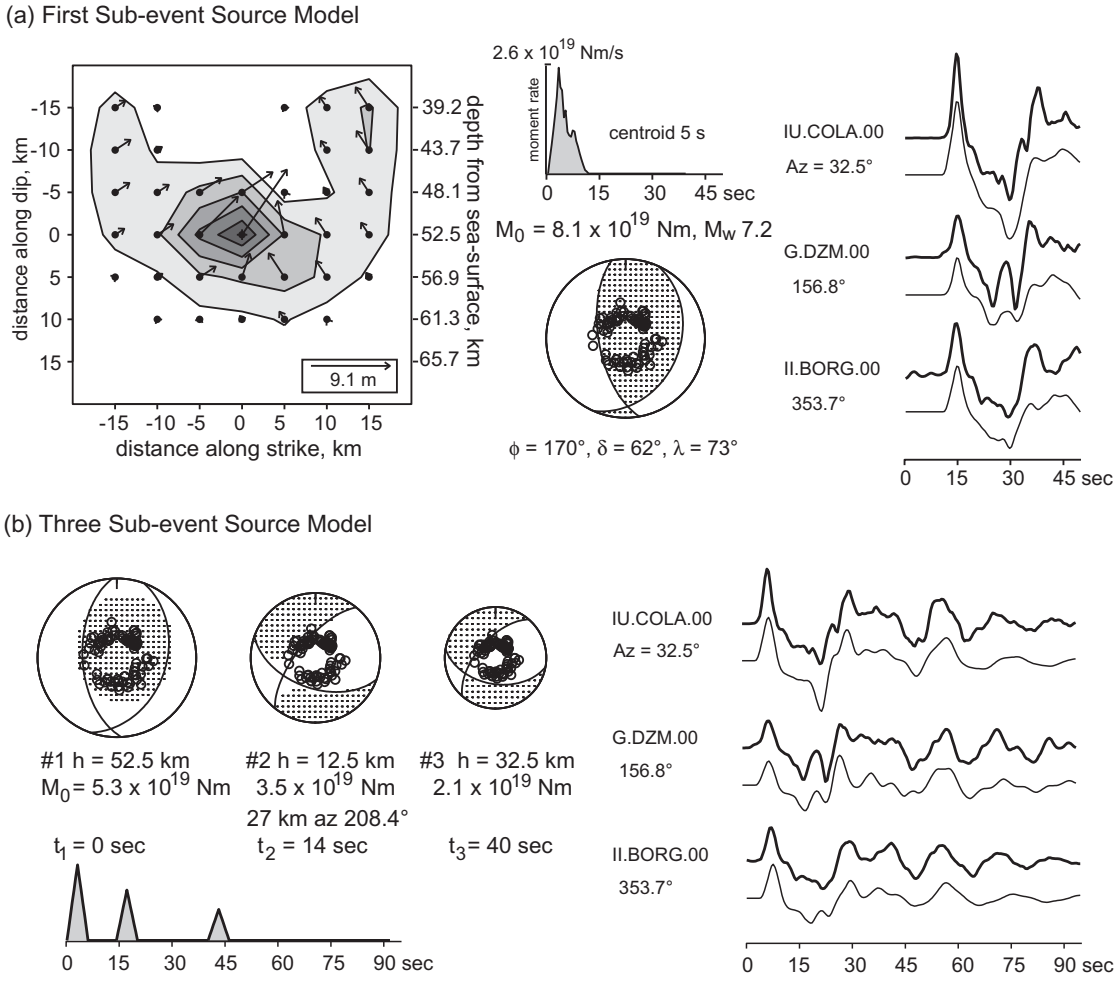

Fig. 3. (a) Finite-fault inversion for the first sub-event of the December 7, 2012 event using the early portion of teleseismic P wave signals. The slip model for a rupture velocity of 3.0 km/s is shown along with the moment-rate function and double-couple focal mechanism (take-off positions of the raypaths to the 87 stations used in the inversion are shown in the focal mechanism). Comparison of representative P wave observations (bold lines) and synthetics (light lines) are shown on the right. (b) Source model from a 3 sub-event iterative deconvolution of 87 P waves for the December 7, 2012 event. The sub-event moment tensors, timing and seismic moments are shown, with the event time sequence indicated on the lower left. Comparison of representative P wave observations (bold lines) and synthetics (light lines) are shown on the right. Additional waveform comparisons for this inversion are shown in Fig. S3.

We used extensive Neighborhood Algorithm sampling of location parameters to evaluate uncertainties (Sambridge, 1999). Formal error estimation is very challenging for complex models, but based on characterizing the spatial domain for which we find solutions with no more than 10% relative increase in RMS residual from the optimal model (See Fig. S2), we estimate epicentral locations with about 25 km radius of uncertainty relative to the solution shown here, and about ±10 km uncertainty in the relative depth estimates for first-event depths compatible with body wave estimates. Research is continuing on how to best estimate posterior probability density functions for multiple parameter solutions like we present here, but the general uncertainty inferences above are consistent with our experience.

The gCMT solution for two moment tensors has basically similar character with a deeper compressional sub-event and a shallower, southwesterly shifted extensional event (Fig. 1). The centroid locations for both the W-phase and gCMT two-point-source models are shifted tens of kilometers oceanward from the NIED centroids of shallow normal-faulting aftershocks, which align along a trend consistent with the strike of all nodal planes. Note that none of the aftershocks have thrust-faulting geometries. Among several hundred aftershocks of the great 2011 Tohoku earthquake near the trench or toward the outer rise, only two small thrust-faulting mechanisms are in the NIED catalog, and those have northerly trending compression axes; other events are normal faulting except for a few oblique strike-slip mechanisms.

Teleseismic broadband P wave observations were inverted for slip distribution for the first of the two mainshock sub-events (Fig. 3a), with no clear preference of fault plane being found. The solution for the westward dipping plane in Fig. 3a has slip concentrated between 50 and 60 km with a source duration of less than 10 s. The spatial resolution of the slip model is limited, but the overall mechanism is very compatible with the first sub-event from the two double-couple W-phase inversion. A multiple sub-event model was required to match the overall P waveforms, with a three moment tensor sub-event solution from iterative deconvolution (Kikuchi and Kanamori, 1991) being shown in Fig. 3b. Each sub-event was parameterized with a triangular source time function with 3-s rise and 3-s fall. The solution indicates a 14 s time shift between the first and second subevents, with the initial deeper thrust being at 52.5 km depth and the shallower normal faulting solution being at 12.5 km depth 27 km to the south–southwest (azimuth of 208.4°). This is very consistent with the two double-couple W-phase inversion. A third subevent begins at 40 s,

with similar mechanism to the normal-fault subevent at 14 s, but at 32.5 km depth. This last sub-event matches strong P arrivals between 45 and 65 s in the P waveforms (Fig. 3b and Supplemental Fig. S3). Searches over a grid of possible secondary event locations indicates that uncertainties in the relative locations are on the order of ±15 km in epicentral separation and several seconds in relative timing. The relative depth uncertainty has trade-offs with mechanism, but appears to be about ±10 km for models we deem within the acceptable range of RMS waveform residual increase from the best fit solution.

As for any complex source model with multiple faulting mechanisms, there are substantial uncertainties and trade-offs in the details of each sub-event, but overall the broadband P wave and W-phase observations are quite well accounted for by the composite mechanisms in Figs. 2b and 3b, and we view these as basic representations of the mainshock process. We are not able to confidently resolve details such as the specific fault planes or stress drops, although the overall P wave energy radiation is typical of relatively high stress drop intraplate faulting, and the USGS energy magnitude $M_e = 8.3$ is unusually large. The relative timing of the first two sub-events strongly indicates triggering of the shallower normal faulting by the deeper thrust faulting, accompanied by activation of the extensive normal faulting aftershocks sequence.

3. Other deep near-trench compressional sequences

The four recent earthquake sequences involving large, relatively deep intraplate thrust-faulting near subduction zone trenches are schematically summarized in Fig. 4. The central Kuril Islands Trench sequence (Fig. 4a) involved a great interplate thrust event (M_w 8.3) on November 15, 2006, followed by a great outer trench slope normal faulting event (M_w 8.1) on January 13, 2007, and two-years later a large deep intraplate thrust event (M_w 7.4) on January 15, 2009 (e.g., Lay et al., 2009). A large intraplate thrust event had occurred in this region in 1963, and was interpreted as indicating build-up of in-plane compressional stress prior to megathrust failure (Christensen and Ruff, 1988). The northern Kermadec Trench region (Fig. 4b) experienced a large (M_w 7.6) normal faulting event on July 6, 2011, which activated both shallow normal faulting and fairly extensive moderate-size interplate thrust faulting, along with a large (M_w 7.4) deep intraplate thrust on October 21, 2006 (Todd and Lay, 2013). The Philippine Trench region (Fig. 4c) experienced a deep trench slope event on August 31, 2012 that activated shallow normal-faulting and a few interplate thrust events (Ye et al., 2012). The Japan Trench region (Fig. 4d) where the 2012 doublet occurred is adjacent to the M_w 9.0 2011 Tohoku underthrusting event and landward of a large (M_w 7.6) shallow normal faulting aftershock about 30 min after the great

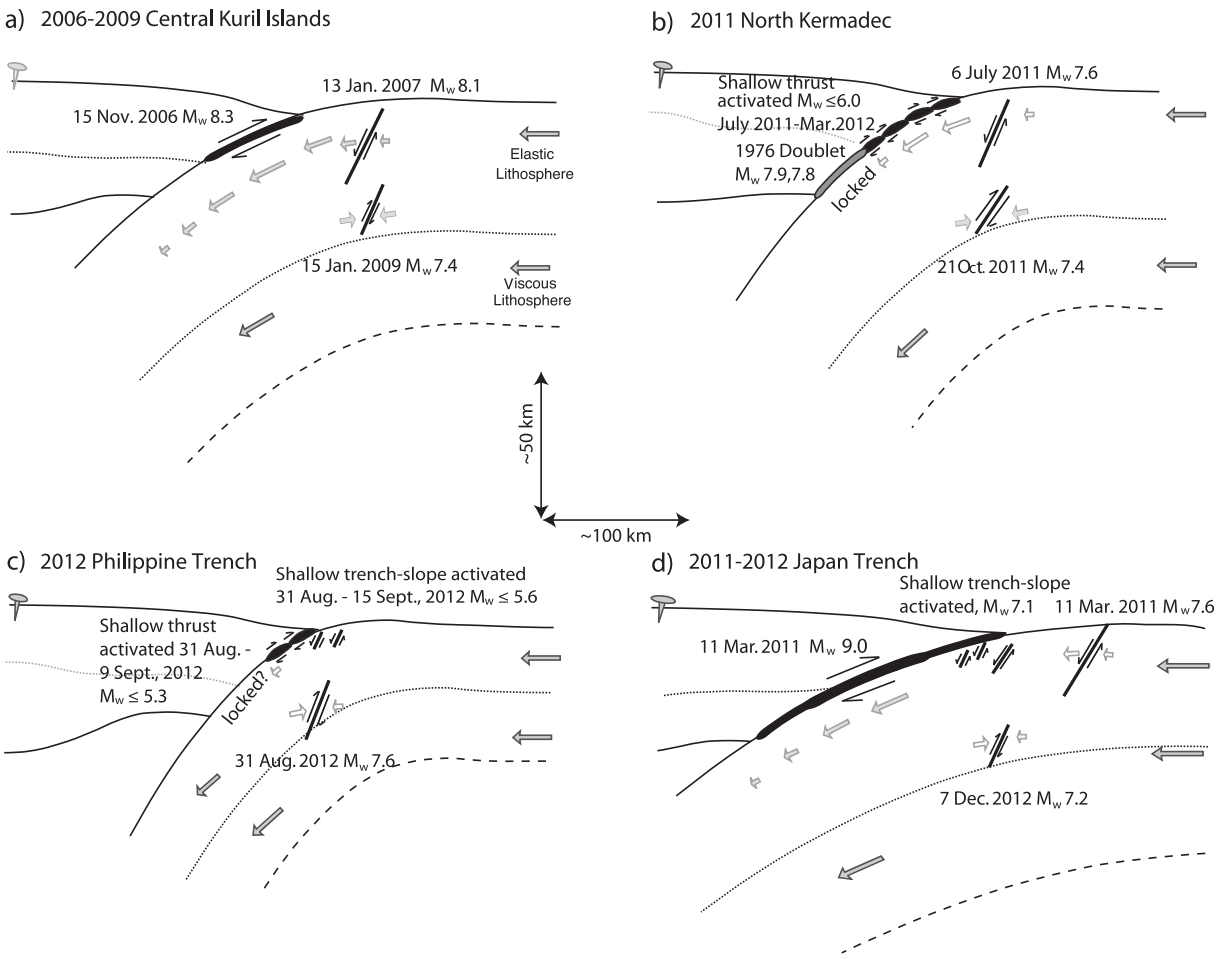

Fig. 4. Schematic cross-sections for the arcs that have recently experienced large below trench thrust faulting events, and related large interplate and intraplate events. All figures have a 2:1 vertical exaggeration, and the panels have the same spatial scale. Note that the deep compressional events increase in size as the curvature of the shallow underthrusting plate increases. The events in each region are not all in a common vertical plane. Figs. S4 and S5 show map views of the gCMT focal mechanisms for each sequence.

event. Map views of the gCMT faulting solutions for these sequences are shown in Figs. S4 and S5 to convey the along-strike variation in these complex sequences.

These sequences suggest stress transfer and activation of multiple fault systems in the shallow interplate and intraplate environments, superimposed on long-term plate bending and convergence deformation. For the Japan Trench sequence we computed Coulomb stress changes on the various fault geometries produced by interplate thrusting, outer rise normal faulting and deep intraplate thrusting, allowing for the ambiguity of fault planes for the intraplate events. For representative slip models of the 2011 Tohoku earthquake we calculate 10–20 bar increases in driving stress on outer rise normal faults (consistent with Lay et al., 2011), with potentially comparable increase in driving stress for deep thrust faulting below the trench. The latter is uncertain due to the unclear nature of strain release in the shallow megathrust region. The deep intraplate thrust sub-event of the 2012 doublet added 2–3 bar driving stress on shallow normal fault geometries near the trench and decreases in driving stress on the near-trench megathrust, consistent with preferential activation of normal faulting aftershocks. Comparable interactions are found for the other sequences, with shallow intraplate normal faulting and deeper intraplate compressional faulting plausibly acting to trigger each fault system, as does large interplate thrusting.

Given that the recent deep intraplate thrusting in the central Kuril Islands and Japan Trenches follows large interplate thrust events, the stress interactions are clearly more complicated than in the end-member seismic cycle model of Christensen and Ruff (1988). Considering the large slip of the 2011 Tohoku earthquake, it may be somewhat surprising that no deep compressional events were observed before that rupture, although only a modest number of great megathrust failures have been preceded by deep compression, including the 2006 Kuril Islands event. The rarity of deep outer rise thrusting still suggests that such events may provide a sensor of in-plate compressional stress accumulation for some regions. Fig. 4 suggests that the degree of curvature of the subducting plate, which is plausibly related to whether there is any unrelaxed plate bending stress, may be a factor in whether deep compressional events occur before megathrust failures. The strong curvature of the Philippine plate may thus be related to the large size of the 2012 thrust event in that region, although there is uncertainty in the state of frictional coupling of the adjacent megathrust (e.g., Ye et al., 2012). The 2011 Kermadec sequence occurred up-dip of a locked portion of the megathrust that last failed in two large thrust events in 1976 (preceded by outer rise compressional and normal faulting events in 1974).

While the number of sequences is limited and each is distinct in nature, our impression is that given the added complexity of strong interactions between shallow and deep faulting environments, it remains reasonable that for subduction zones with strong slab curvature, the presence of unrelaxed compressional stress in the near-trench intraplate environment may enhance sensitivity to the interplate seismic stress cycle. The extensive outer rise normal faulting activity of the 2011 Tohoku aftershock sequence suggests that the low curvature of the Japan slab leads to dominance of shallow extensional stresses in response to the megathrust rupture, with deep thrust faulting as in the 2012 doublet only occurring as a result of stress increments from the megathrust failure and from large normal fault ruptures. Future modeling of faulting in slabs with different curvature and rheological properties may be able to quantify these tendencies. This leaves open the potential for very large normal faulting like that of the 1933 Sanriku earthquake to occur in the Tohoku outer trench slope region (Lay et al., 2011), compounding the risk of damaging tsunami along the Honshu coastline.

Acknowledgments

This work made use of GMT, matplotlib, SAC and Coulomb 3.0 software. The IRIS DMS data center was used to access the seismic data from Global Seismic Network and Federation of Digital Seismic Network stations. We thank Editor G. Helffrich and an anonymous reviewer for their helpful suggestions. This work was supported by NSF grants EAR-1245717 (T.L.).

Appendix A. Supplementary data

Supplementary data associated with this article can be found, in the online version, at http://dx.doi.org/10.1016/j.pepi.2013.04.009.

References

Christensen, D.H., Ruff, L.J., 1988. Seismic coupling and outer rise earthquakes. J. Geophys. Res. 93 (B11), 13421–13444.

Duputel, Z., Kanamori, H., Tsai, V.C., Rivera, L., Meng, L., Ampuero, L.J.-P., Stock, J.M., 2012. The 2012 Sumatra great earthquake sequence. Earth Planet. Sci. Lett. 351–352, 247–257.

Hino, R., Azuma, R., Ito, Y., Yamamoto, Y., Suzuki, K., Tsushima, H., Suzuki, S., Miyashita, M., Tomori, T., Arizono, M., Tange, G., 2009. Insight into complex rupturing of the immature bending normal fault in the outer slope of the Japan Trench from aftershocks of the 2005 Sanriku earthquake (M_w = 7.0) located by ocean bottom seismometry. Geochem. Geophys. Geosyst. 10, Q07018. http://dx.doi.org/10.1029/2009GC002415.

Huang, Z., Zhao, D., 2013. Relocating the 2011 Tohoku-oki earthquakes (M 6.0–9.0). Tectonophysics 586, 35–45.

Kanamori, H., Rivera, L., 2008. Source inversion of W-phase: speeding up seismic tsunami warning. Geophys. J. Int. 175, 222–238.

Kikuchi, M., Kanamori, H., 1991. Inversion of complex body waves III. Bull. Seismol. Soc. Am. 81, 2335–2350.

Lay, T., Astiz, L., Kanamori, H., Christensen, D.H., 1989. Temporal variation of large intraplate earthquakes in coupled subduction zones. Phys. Earth Planet. Inter. 54, 258–312.

Lay, T., Kanamori, H., Ammon, C.J., Hutko, A.R., Furlong, K., Rivera, L., 2009. The 2006–2007 Kuril Islands great earthquake sequence. J. Geophys. Res. 114, B11308. http://dx.doi.org/10.1029/2008JB006280.

Lay, T., Ammon, C.J., Kanamori, H., Kim, M.J., Xue, L., 2011. Outer trench-slope faulting and the 2011 M_w 9.0 off the Pacific coast of Tohoku earthquake. Earth Planet. Space 63, 713–718.

Li, X., Ji, C., 2013. 2012 MS 7.3 Honshu earthquake: earthquake doublet with different focal mechanisms, (abstract). Seismol. Res. Lett. 84 (2).

Obana, K., Fujie, G., Takahashi, T., Yamamoto, Y., Nakamura, Y., Kodaira, S., Takahashi, N., Kaneda, Y., Shinohara, M., 2012. Normal-faulting earthquakes beneath the outer slope of the Japan Trench after the 2011 Tohoku earthquake: implications for the stress regime in the incoming Pacific Plate. Geophys. Res. Lett. 39, L00G24. http://dx.doi.org/10.1029/2011GL050399.

Sambridge, M., 1999. Geophysical inversion with a neighborhood algorithm – I. Searching a parameter space. Geophys. J. Int. 138, 479–494.

Todd, E.K., Lay, T., 2013. The 2011 Northern Kermadec earthquake doublet and subduction zone faulting interactions. J. Geophys. Res. 118, 1–13. http://dx.doi.org/10.1029/2012JB009711.

Ye, L., Lay, T., Kanamori, H., 2012. Intraplate and interplate faulting interactions during the August 31, 2012 Philippine Trench earthquake (M_w 7.6) sequence. Geophys. Res. Lett. 39, L24310. http://dx.doi.org/10.1029/2012GL054164.